

# Dilepton production in proton-proton reaction at 4.5 GeV with the HADES spectrometer

Rayane Abou Yassine<sup>1,2,\*</sup> for the HADES collaboration

<sup>1</sup>Laboratoire de Physique des 2 infinis Irène Joliot-Curie, Université Paris-Saclay, CNRS-IN2P3., F-91405 Orsay, France

<sup>2</sup>Technische Universität Darmstadt, 64289 Darmstadt, Germany

**Abstract.** Spectra of dileptons emitted in hadron collisions are important tool to study electromagnetic decays of resonances and the validity of the Vector Meson Dominance model. Furthermore, they provide reference spectra for the hot and dense (heavy-ion A+A collisions) and cold nuclear matter (p+A collisions). In February 2022, proton-proton reactions at 4.5 GeV beam kinetic energy were measured by HADES experiment. The aim of the analysis is to study the specific channels that produced dileptons, such as baryonic resonance Dalitz decays ( $\Delta/N^* \rightarrow Ne^+e^-$ ) and vector meson decays ( $\rho/\omega/\varphi \rightarrow e^+e^-$ ). In addition, the investigations of dielectron production above the  $\varphi$  meson mass will be enabled. In this contribution, different steps of the  $e^+e^-$  pair reconstruction are discussed.

## 1 Introduction

### 1.1 Physics motivation

Dileptons ( $e^+e^-$  pairs produced in decays of virtual photons) are crucial probes of processes occurring in hadronic and heavy-ion collisions. By studying the former, it is possible to understand the electromagnetic structure of baryonic transitions in the time-like region where the four-momentum squared  $q^2 = M_{ee}^2$  is positive. It is complementary to the space-like region ( $q^2 < 0$ ) probed in electron scattering processes measured with the CLAS detector at JLab [1]. In particular, baryon Dalitz decays are highly relevant to investigate the validity of the Vector Meson Dominance (VMD) model in electromagnetic transitions of baryons, as at large positive  $q^2$ , the  $\rho$  and  $\omega$  vector mesons are expected to play a significant role. In addition, the yield above the  $\varphi$  mass ( $M_{e^+e^-} > 1020 \text{ MeV}/c^2$ ) is interesting to search for chiral symmetry restoration signals [2]. The spectroscopy of  $e^+e^-$  pairs is also an ideal probe to study the in-medium effects on the vector meson properties in heavy-ion collisions since they do not interact strongly when propagating through hadronic matter, therefore they have a free mean path larger than the system size and can reflect the whole history of the collision [3]. The investigation of elementary reactions such as p+p and p+n provide useful reference spectra for the analyses of heavy-ion collisions in order to quantify the in-medium effects. Figure 1 shows the inclusive  $e^+e^-$  spectrum in nucleon-nucleon reaction used as reference for Au+Au collision at the same energy measured by HADES [4]. This reference

\*e-mail: rayane.abou-yassine@ijclab.in2p3.fr

allows to determine cross sections for the meson production and to investigate the spectral function of the broad  $\rho$  meson, which is sensitive to the coupling to baryon resonances.

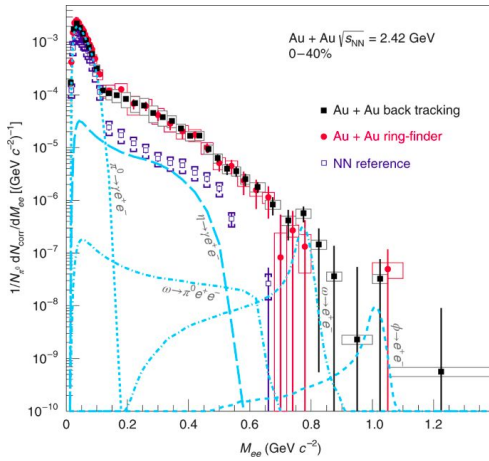


**Figure 1.** Di-electron invariant mass spectrum in Au+Au collisions at  $\sqrt{s} = 2.42$  GeV (black squares and red dots) and the NN reference at the same energy (violet squares) measured by HADES. The curves show simulations for the different long living  $e^+e^-$  sources [4].

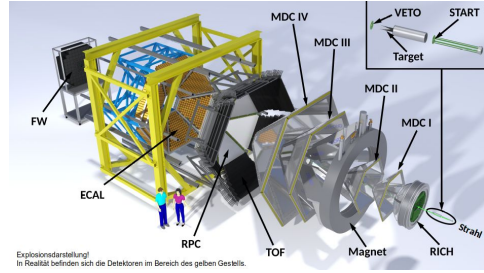


**Figure 2.** Schematic view of the HADES detector with different sub-detectors (see sec. 1.2).

Several pp measurements at incident energies of 1-3.5 GeV/nucleon were performed with the HADES spectrometer. The pp reactions at 1.25 GeV beam kinetic energy were studied for a better understanding of the contribution of  $\Delta$ -Dalitz decay and NN bremsstrahlung processes to dielectron production in heavy-ion collisions. The detailed analysis of the exclusive  $pp \rightarrow ppe^+e^-$  channels allowed to extract the branching ratio of the  $\Delta(1232)$  Dalitz decay for the first time [5] and has been included in the review of the Particle Data Group [6]. In pp collisions at 3.5 GeV/nucleon energy, the inclusive production cross sections for neutral pions,  $\eta$ ,  $\omega$  and  $\rho$  mesons were determined from dielectron experimental data [7], while the exclusive analysis allowed for a selective study of baryon Dalitz decay and vector meson ( $\rho/\omega$ ) decays, and significant effects related to the electromagnetic Transition Form-Factors ( $eTFF$ ) could be observed [8]. Specific study of VMD effects was performed also using a pion beam experiment [9]. Recently, HADES measured pp collisions at 4.5 GeV/nucleon beam kinetic energy, and preliminary results from the inclusive  $e^+e^-$  analysis will be discussed in section 2. HADES analyses help to understand the microscopic structure of baryon rich matter where the baryonic resonances play an important role. They are complementary to the studies made by LHC, SPS, RHIC experiments that are interested in the region of high temperatures and low baryochemical potential.

## 1.2 HADES experimental setup

The HADES (High Acceptance Di-Electron Spectrometer) is a fixed target experiment located at GSI, Darmstadt, Germany. It was designed for the identification and invariant mass reconstruction of electron-positron pairs ( $e^+e^-$ ), decays of light vector mesons in elementary and in heavy-ion collisions. HADES detector is a magnetic spectrometer consisting of six

identically designed sectors with a large geometrical acceptance [10], allowing for a coverage of the full azimuthal angle range and polar angles between  $18^\circ$  and  $85^\circ$ , as shown in figure 2. The particle momentum is determined with the tracking system, formed by four low-mass Mini-Drift Chamber (MDC) planes located in front and behind the magnet, that measures the deflection angle of the particle trajectories in the magnetic field. The lepton identification is performed with the Ring Imaging Cherenkov (RICH) detector, together with the Electromagnetic Calorimeter (ECAL) and the time of flight detectors (RPC for  $\theta < 45^\circ$  and TOF for  $\theta > 45^\circ$ ). The Forward detector (FW) is a new setup consists of two Straw Tracking Stations and a Forward Resistive Plate Chamber (FRPC) detector for the time of flight measurements and allows the measurement of particles at small polar angles ( $0.5^\circ < \theta < 7^\circ$ ).

## 2 Proton-proton collisions at 4.5 GeV

In February 2022, an experiment took place using a proton beam with a kinetic energy of 4.5 GeV/nucleon on a liquid hydrogen target. One of the main components of the detector serving for electron and positron selection is the hadron-blind Ring-Imaging Cherenkov detector (RICH). To increase the purity of the selection at high momenta, ECAL information is used as will be discussed in the following sections. The analysis will be enhanced by using the information from time-of-flight detectors after their calibration will be completed. In this inclusive  $e^+e^-$  analysis, around 16.8 billion of events were used.

### 2.1 Information from the RICH detector

The RICH detector is based on the Cherenkov effect: a charged particle with velocity larger than the speed of light in a given medium creates a Cherenkov light emitted in a cone. The photons are then reflected by the RICH mirror and form a ring on the photon detector. The pa-

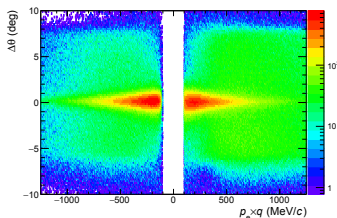


**Figure 3.**  $\Delta\theta$  of the particle vs. its momentum times charge.

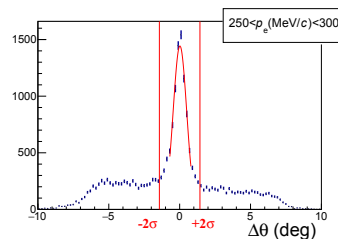


**Figure 4.**  $\Delta\theta$  distribution of electrons for one momentum bin with fitted peak by Gaussian.

rameters used to select lepton tracks are the difference  $\Delta\theta$  ( $\Delta\phi$ ) between the polar (azimuthal) angle of the track and the ones of the ring. The  $\Delta\theta$  distribution vs. the particle momentum is presented in figure 3. The  $\Delta\theta$  distribution shows a background under the lepton peak (see figure 4). It is due to random matches between a ring in the RICH and a track in the MDC. The strategy to select lepton candidates is to make projections for different momentum bins, fit the peak by a Gaussian and keep events in a  $\pm 2\sigma$  region around its centre as showed in figure 4. Same strategy is followed for  $\Delta\phi$  distributions.

### 2.2 Information from the ECAL detector

The ECAL information matched spatially with the track is also checked to improve the purity of lepton candidate selection. The type of the detected particles is identified using the

difference between the deposited energy of each particle ( $E$ ) in the ECAL and the energy calculated from its reconstructed momentum ( $p$ ) assuming zero mass. Leptons leave most of their energies in the calorimeter material while hadrons leave smaller fraction. Thus the quantity  $(E - pc)$  should be around zero for leptons and negative for hadrons. A two-dimensional representation of  $(E - pc)$  versus momentum is shown in figure 5 where tracks with negative values are not fully suppressed after RICH cuts (section 2.1). The  $(E - pc)$  peak around zero is fitted with a Gaussian and leptons with  $(E - pc) \geq -3\sigma$  are selected (see figure 6). In this way, the purity of the lepton selection can be improved at the highest momenta.

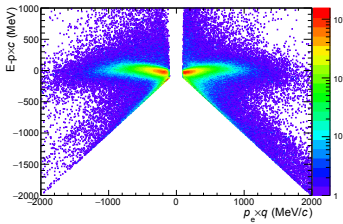


**Figure 5.** Difference between the deposited energy in the ECAL of a particle and its momentum after RICH cuts in function of momentum times charge.

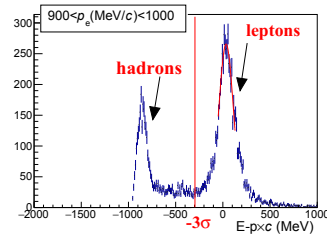


**Figure 6.**  $(E - pc)$  distribution for positrons for one momentum bin with fitted peak by Gaussian.

### 2.3 $e^+e^-$ invariant mass spectrum

After the selection of electron and positron candidates, they are combined into pairs that correspond to virtual photons. Unfortunately, there is no available information to distinguish the correlated pairs that originate from the same electromagnetic vertex (same virtual photon), from uncorrelated pairs which constitute the combinatorial background (CB) and have to be suppressed. Two categories of combinatorial background are distinguished. The correlated background originating mostly from the  $\pi^0$  decay into two photons or its Dalitz decay, and a subsequent photon conversion. In this case, it is possible to have a lepton pair originating from a different virtual photon, but from the same decaying particle as shown in figure 7 (left panel). Besides, the un-correlated combinatorial background is created by random combinations between leptons originating from two independent sources as presented in figure 7 (right panel).

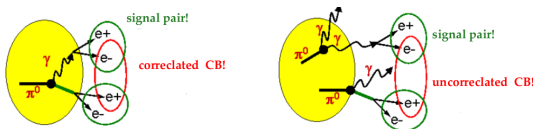


**Figure 7.** Schematic view of the correlated (left panel) and un-correlated (right panel) combinatorial background.

The CB is estimated by the geometrical mean formula of like-sign  $e^+e^+$  ( $N_{++}$ ) and  $e^-e^-$  ( $N_{--}$ ) pairs [11]:

$$CB_{+-} = 2 \sqrt{N_{++}N_{--}}$$

A strong contribution to the CB arises from the conversion of real photons in the target and detector material, it is therefore important to suppress it as much as possible. These pairs are characterized by small opening angles. Therefore, a partner of a conversion pair is identified

in the analysis if the ring has a high number of hits in the photon detector which characterizes overlapping rings from conversion pairs [12], or if a nearby track segment, in a cone of  $4^\circ$  is found in the inner detectors. These two conditions were labelled as "RingCut" and "TrackCut" respectively. Such tracks are removed from the sample and hence do not contribute to the CB. Finally, after CB subtraction, only pairs with opening angle larger than  $9^\circ$  are kept, to fully suppress the conversion contamination. Figure 8 presents a comparison of the signal to background ratio with the different conversion rejection cuts. Figure 9 shows the invariant mass distribution of all  $e^+e^-$  combinations, the CB estimated and the signal of correlated pairs resulting from the CB subtraction. Peaks corresponding to  $\omega$  and  $\varphi$  mesons are clearly visible in the spectrum. The high statistics enable the measurement of the inclusive cross section for  $\omega$  meson production where the number of particles produced is estimated between 16000 and 20000. However, detailed simulations are needed to determine the contribution of the  $\rho$  meson to the  $\omega$  yield and then calculate its cross section.

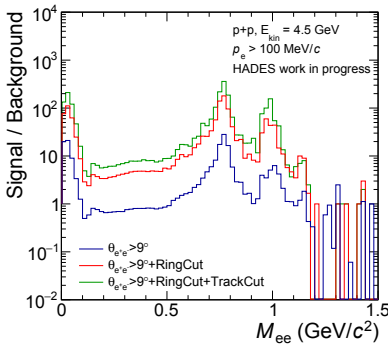


**Figure 8.** Measured signal to combinatorial background ratio for the different cuts used to reject leptons from real photon conversion as explained in 2.3.

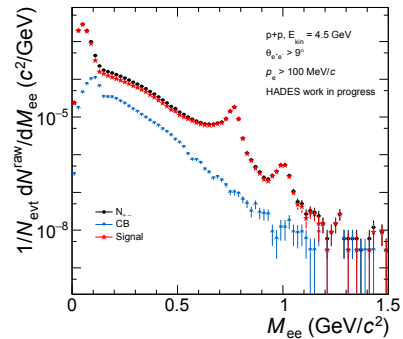


**Figure 9.** Inclusive  $e^+e^-$  invariant mass spectrum in p+p collisions at 4.5 GeV beam kinetic energy measured by HADES.

## 2.4 Study of $\eta \rightarrow e^+e^-$ decay

The HADES collaboration established the upper limit of the branching ratio for the rare  $\eta$  meson direct decay into  $e^+e^-$  using data on dielectron emission in proton induced reactions on a Nb target at 3.5 GeV/nucleon beam kinetic energy. It was set at  $2.3 \times 10^{-6}$  [13]. The VEPP-2M collaboration studied also this rare decay using the inverse reaction  $e^+e^- \rightarrow \eta$  with SND detector in the center of mass energy range 520-580 MeV, and lowered this limit to  $7 \times 10^{-7}$  [14]. The statistics for p+p with HADES at 4.5 GeV are promising to improve this branching ratio upper limit (see figure 10).

## 3 Conclusion and outlook

The study of dielectron spectroscopy in p+p collisions at 4.5 GeV with HADES was presented. The selection of lepton candidates is performed by a combination of information from the RICH ( $\Delta\theta, \Delta\phi$ ) and ECAL (deposited energy) detectors. Lepton selection will be further improved using the time-of-flight information. The combinatorial background is

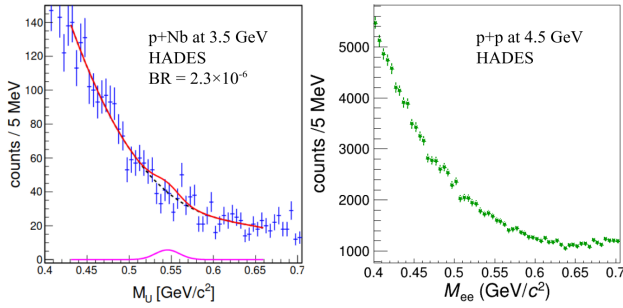


**Figure 10.**  $e^+e^-$  invariant mass spectrum in the mass region of  $\eta$  in p+Nb at 3.5 GeV [13] (left panel) and in p+p at 4.5 GeV (right panel) measured by HADES.

reduced due to appropriate cuts adjusted to suppress tracks originating from close pairs. The preliminary results are promising: the high recorded statistics will be beneficial to determine the cross section for  $\omega$  production and to possibly improve the upper limit of the branching ratio for  $\eta \rightarrow e^+e^-$  decay. Simulations based on models (Pluto, SMASH, UrQMD, GiBUU) will be used for the comparison to data.

We acknowledge support from SIP JUC Cracow, Cracow (Poland), National Science Center, 2016/23/P/ST2/040 POLONEZ, 2017/25/N/ST2/00580, 2017/26/M/ST2/00600; TU Darmstadt, Darmstadt (Germany), DFG GRK 2128, DFG CRC-TR 211, BMBF:05P18RDFC1, HFHF, ELEMENTS:500/10.006, VH-NG-823, GSI F&E, ExtreMe Matter Institute EMMI at GSI Darmstadt; Goethe-University, Frankfurt (Germany), BMBF:05P12RFGHJ, GSIF&E, HIC for FAIR (LOEWE), ExtreMe Matter Institute EMMI at GSI Darmstadt; TU München, Garching (Germany), MLL München, DFG EClust 153, GSI TMLRG1316F, BmBF 05P15WOFCA, SFB 1258, DFG FAB898/2-2; JLU Giessen, Giessen (Germany), BMBF:05P12RGGHM; IJCLab Orsay, Orsay (France), CNRS/IN2P3, P2IO Labex, France; NPI CAS, Rez, Rez (Czech Republic), MSMT LM2018112, LTT17003, MSMT OP VVV CZ.02.1.01/0.0/0.0/18 046/0016066.

## References

- [1] V. I. Mokeev *et al.* Phys. Rev. C **108**, no.2, 025204 (2023).
- [2] U. Mosel, *Fields, Symetries and Quarks* (Springer, Berlin, 1999).
- [3] G. Agakichiev *et al.* CERES collaboration, Phys. Rev. Lett. **75**, 1272-1275 (1995).
- [4] J. Adamczewski-Musch *et al.* HADES collaboration, Nature Phys. **15** 1040-1045 (2019).
- [5] J. Adamczewski-Musch *et al.* HADES collaboration, Phys. Rev. C **95**, 065205 (2017).
- [6] M. Tanabashi *et al.* (Particle Data Group), Phys. Rev. D **98**, 030001 (2018).
- [7] G. Agakishiev *et al.* HADES collaboration, Eur. Phys. J. A **48**, 64 (2012).
- [8] G. Agakishiev *et al.* HADES collaboration, Eur. Phys. J. A **50**, 82 (2014).
- [9] R. Abou Yassine *et al.* HADES collaboration, (2023), [arXiv:2309.13357 [nucl-ex]].
- [10] G. Agakishiev *et al.* HADES collaboration, Eur. Phys. J. A **41**, 243-277 (2009).
- [11] M. Gazdzicki and M. I. Gorenstein, (2000), [arXiv:hep-ph/0003319 [hep-ph]].
- [12] J. Otto, PhD thesis, Justus Liebig University Giessen, (2022).
- [13] G. Agakishiev *et al.* HADES collaboration, Phys. Lett. B **731**, 265 (2014).
- [14] M. N. Achasov *et al.* SND collaboration, Phys. Rev. D **98**, 052007 (2018).